INDIAN INSTITUTE OF SCIENCE

CENTRE FOR NANO SCIENCE AND ENGINEERING (CeNSE)

NE240 : MATERIALS DESIGN PRINCIPLES FOR ELECTRONIC, ELECTROMECHANICAL AND OPTICAL FUNCTIONS

Term Paper

Topological Insulators and Topological Phase Transitions

Chaitali Shah
(SR No: 01-02-04-10-51-21-1-19786)

Date: November 29, 2023

Abstract

This term paper introduces the idea of topological materials and associated symmetries. The phase transition to the topological phase is explained using the Su-Schrieffer-Heeger model. The winding number is explained as the topological invariant for this case. The paper presents a phase transition from a normal insulator to a topological metal. This is studied by understanding the hidden symmetry of the quasi 1-D lattice proposed along with other parameters like the band diagram and topological invariants. The numerical results that prove the emergence of the topological metallic phase using inverse participation ratios and local density of state are discussed. This is followed by the general outline of the history of 2D and 3D topological insulators and the experimental techniques used to detect them. The term paper concludes with some applications and the future scope of this area.

Introduction

In the course NE240, we learned about phases that can be understood using Landau theory, which characterises states based on the underlying spatial symmetries and the breaking of these symmetries. In the past decade, the discovery and research on topological materials (starting with the Quantum Hall effect) has led to a new classification paradigm based on the idea of *topological order*. The classification of symmetry groups is done based on the symmetry properties of $\mathcal{H}(k)$, the Hamiltonian in the momentum space. $\mathcal{H}(k)$ can possess three kinds of symmetry - time-reversal symmetry (T), particle-hole symmetry (P) and chiral symmetry (C). Based on this concept, materials are classified into ten discrete symmetry classes. This idea is analogous to the classification of materials, based on spatial symmetry into 32 point groups and 230 space groups.

A topological insulator is an insulator that possesses a metallic boundary when placed next to an ordinary insulator (equivalent to a vacuum). The bulk has a band gap, but the edge supports a conducting state protected by time-reversal symmetry. These conducting boundaries originate from topological invariants, which cannot change as long as a material remains insulating. In a topological insulator, the electron's wave function is knotted as it moves through momentum space. The topological invariant associated with the knotted case cannot change to that of the simple loop (for the ordinary insulator) without passing through a metallic phase.

Topological Phase Transition in the Su–Schrieffer–Heeger Model

The Su–Schrieffer–Heeger (SSH) model is a 1-dimensional lattice model that displays a topological phase transition. The model consists of N unit cells with two sub-lattices per unit cell as shown in Fig. 2
The Hamiltonian of the system, using the tight-binding theory, is written as follows.

$$H = \sum_{n=1}^{N} t_1 (A_n^\dagger B_n) + \sum_{n=1}^{N-1} t_2 (B_n^\dagger A_{n+1})$$

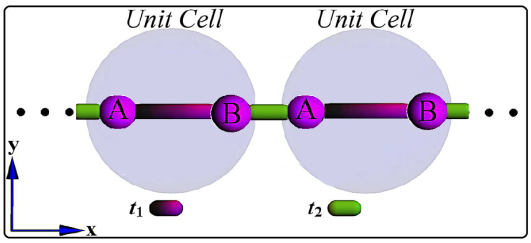

Figure 1: Schematic geometry of 1D lattice in the SSH model

Here, $X_n^\dagger$ is the creation operator, and X_n is the annihilation operator on the sub-lattice $X(=A,B)$ of the n^{th} unit cell. t_1 is the intra-unit cell hopping, and t_2 is the inter-unit cell hopping.

On applying Fourier transform to the above equation, we obtain the Hamiltonian in k-space as follows.

$$\mathcal{H}(k) = \begin{pmatrix} 0 & t_1 + t_2 e^{ik} \\ t_1 + t_2 e^{-ik} & 0 \end{pmatrix}$$

It can be decomposed in terms of Pauli matrices σ_x and σ_y as shown.

$$\mathcal{H}(k) = (t_1 + t_2 cos(k))\sigma_x + (t_2 sin(k))\sigma_y = d_x\sigma_x + d_y\sigma_y$$

The eigenvalues of the Hamiltonian are

$$E^{\pm} = \pm\sqrt{t_1^2 + t_2^2 + 2t_1 t_2 cos(k))}$$

A topological phase transition is possible via the closing and reopening of the bands.

$$E^+ = E^- \text{ when } \; t_1 = t_2$$

When the above condition is met, a topological phase transition may occur. To identify the transition, we have to look at the topological invariant of both the phases.

Winding number The topological invariant in the SSH model is the Winding number. The path of (d_x, d_y) in the $d_x - d_y$ plane as k moves across the Brillouin zone traces out a closed circle of radius t_2 centred at $(t_1, 0)$. The winding number is the number of times the loop winds around the origin of the $d_x - d_y$ plane.

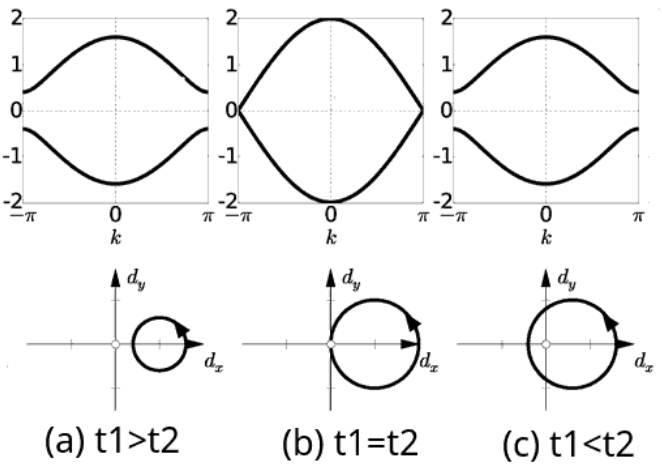

Figure 2: Band structure of the system and path of (d_x, d_y) for (a) $t_1 > t_2$, (b) $t_1 = t_2$ and (C) $t_1 < t_2$

For the SSH model, the winding number is either 0 or 1, depending on the parameters. In the trivial case, when the intra-cell hopping dominates the inter-cell hopping, $t_1 > t_2$, the winding number is 0. In this case, the material is an ordinary insulator. In the topological case, when $t_2 > t_1$, we have the winding number to be 1. The winding number indicates the number of edge states per edge of the material. The change in the winding number indicates the phase transition.

Topological phase transition between a normal insulator and a topological metal state in a quasi-one-dimensional system

The paper under study presents theoretical evidence for a novel phase transition between an ordinary insulator and a topological metal state in a quasi-one-dimensional system. The lattice

considered has N unit cells with three sub-lattices per unit cell, as shown in Fig. 3.

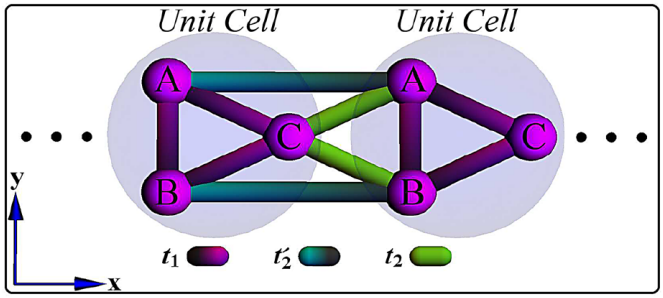

Figure 3: Schematic geometry of quasi-1D lattice

The Hamiltonian of the system is written using the tight-binding theory.

$$H = \sum_{n=1}^{N} t_1(A_n^\dagger B_n + B_n^\dagger C_n + A_n^\dagger C_n) + \sum_{n=1}^{N-1} t_2'(A_n^\dagger A_{n+1} + B_n^\dagger B_{n+1}) + \sum_{n=1}^{N-1} t_2(C_n^\dagger A_{n+1} + C_n^\dagger B_{n+1})$$

Here, $X_n^\dagger$ is the creation operator, and X_n is the annihilation operator on the sub-lattice $X(= A, B, C)$ of the n^{th} unit cell. t_1 is the intra-unit cell hopping and t_2 and t_2' are the inter unit cell hoppings. They are set as multiples of a parameter t, which has the units of energy.

The Hamiltonian is invariant under translations with periodic boundary conditions. The Hamiltonian can be written in the momentum basis ($\psi_k^\dagger = (A_k, B_k, C_k)^\dagger$) after the Fourier transformation.

$$\mathcal{H}(k) = \begin{pmatrix} 2t_2'cos(k) & t_1 & t_1 + t_2e^{ik} \\ t_1 & 2t_2'cos(k) & t_1 + t_2e^{ik} \\ t_1 + t_2e^{-ik} & t_1 + t_2e^{-ik} & 0 \end{pmatrix}$$

The eigenvalues are obtained as follows.

$$E^0 = -2t_1 + \eta$$

$$E^\pm = \frac{1}{2}(\eta \pm \sqrt{\eta^2 + 2(t_1^2 + 4t_2'^2 + 8t_1t_2cos(k))}$$

$$\text{where } \eta = t_1 + 2t_2'cos(k)$$

Topological phases can emerge through closing or reopening of the bands at $k = (0, \pi)$ if $E^+ = E^-$. This condition is met when,

$$t_1 = e^{ik}\frac{2}{9}\left(t_2' + 4t_2 \pm \frac{\sqrt{-(-2t_2' + t_2)^2}}{2}\right)$$

Setting the quantity under the square root to be zero and simplifying the equation leads to the result that topological transition is possible when,

$$t_2' = \frac{t_2}{2} \text{ and } t_1 = e^{ik}t_2$$

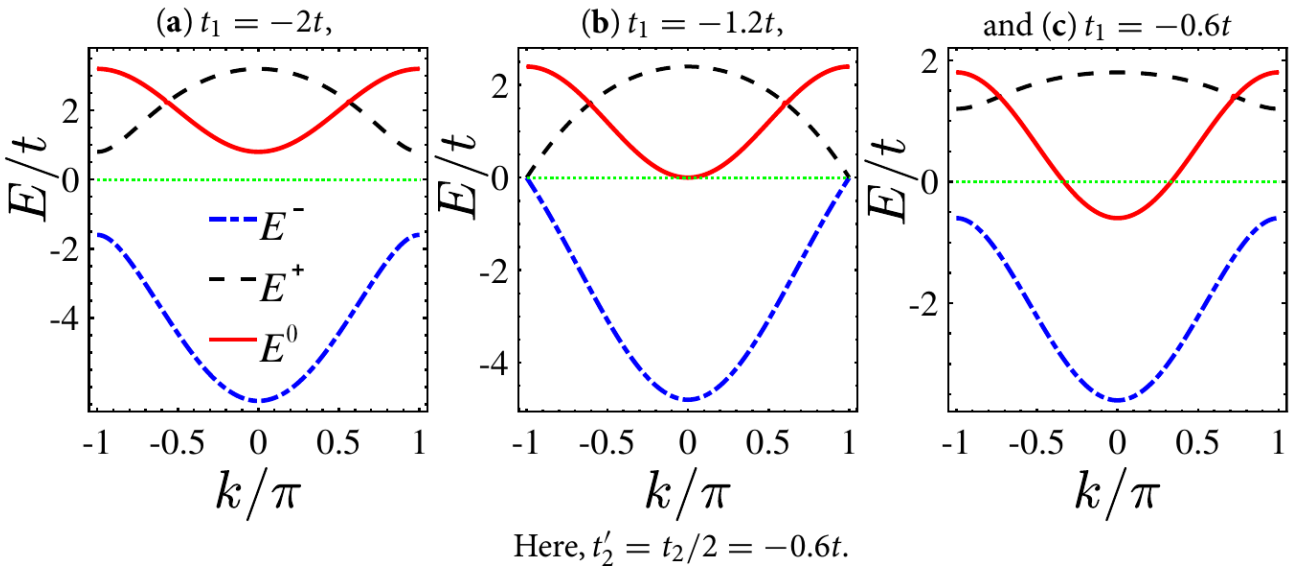

Figure 4: Band structure of the system for (a) $t_1 = -2t$, (b) $t_1 = -1.2t$ and (C) $t_1 = -0.6t$ when $t_2' = \frac{t_2}{2} = -0.6t$. The green line shows the Fermi level

The closing and reopening of bands can be clearly seen in Fig. 4 near the topological phase transition point. In (a), the gap is open, and the material is an insulator, as no states exist near the Fermi level. In (b), at the topological phase transition point, the band gap closes and the band E^0 touches the Fermi level. In (c), the band gap reopens, but the band E^0 crosses the Fermi level representing a conducting state. This indicates that the material transitioned from a normal insulator to a topological metal. Practically, tuning of the hoppings is achieved by = externally applied periodic fields using the Floquet-Bloch theory.

The Hamiltonian has an exchange symmetry with the operator defined as $\Upsilon\psi_k = \psi_k' = (B_k, A_k, C_k)^t$ which exchanges sub-lattice A and B. The Hamiltonian can be block-diagonalised by using the unitary transformation associated with the symmetry operator to obtain,

$$\mathcal{H}(k) = \begin{pmatrix} h_1 & 0 \\ 0 & h_2 \end{pmatrix} \text{ where } h_1 = -2t_1 + \eta \ , \ h_2 = \begin{pmatrix} \eta & \sqrt{2}(t_1 + t_2 e^{ik}) \\ \sqrt{2}(t_1 + t_2 e^{-ik}) & 0 \end{pmatrix}$$

The subsystem h_2 represents a generalised SSH model and can host topological phases which along with the metallic subspace of h_1 makes the overall material a topological metal. There exists a hidden inversion symmetry in the system that protects the topological phase.

Topological invariants The topological invariant for this system is defined as

$$Z = \begin{cases} 0, \text{if } sgn(\eta(0)) = sgn(\eta(\pi)) \\ 1, \text{if } sgn(\eta(0)) \neq sgn(\eta(\pi)) \end{cases}$$

where $sng(x)$ is the Sign function. $\mathcal{Z} = 1$ for a non-trivial topological phase and and $\mathcal{Z} = 0$ for the trivial case. The topological invariant can be seen as a kind of order parameter to determine the phase of the material. It also needs to be mentioned here that, unlike the order parameter, the topological invariant cannot be used to study the transition order.

Discussion of the results

Inverse Participation Ratio The inverse participation ratio for an eigenstate $\psi_E(j)$ of energy E is defined as

$$I_E = \frac{Ln\sum_j |\psi_E(j)|^4}{Ln(3N)}$$

I_E=0 if the eigenstate is localized and I_E=-1 is the eigenstate is extended.

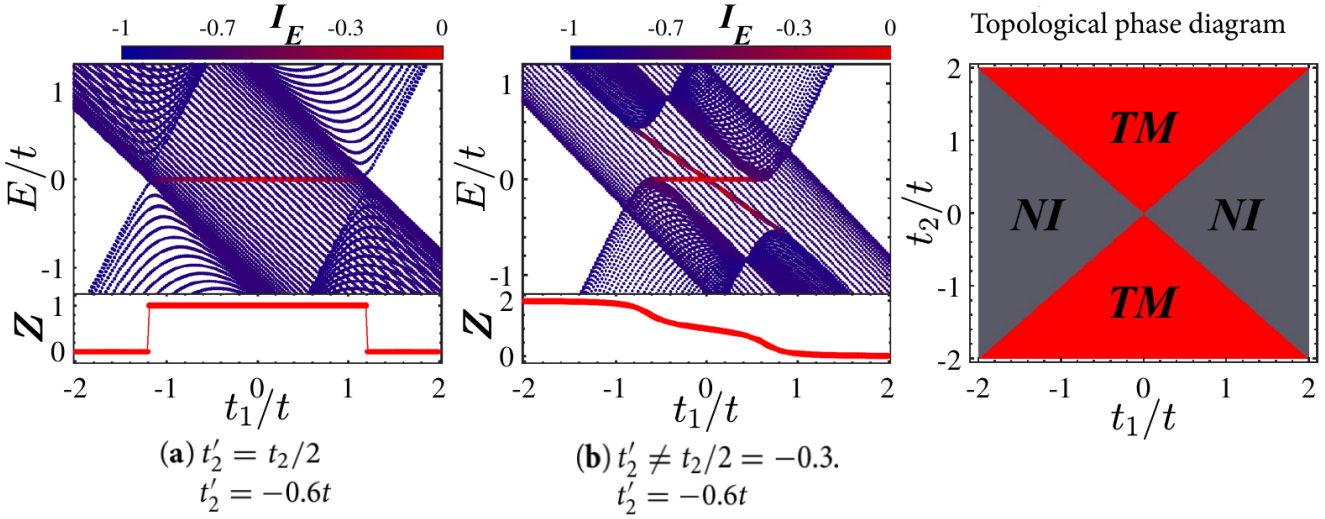

Figure 5: Energy spectra and inverse participation ratio with the topological invariant as a function of t_1/t for (a) $t_2^{'2} = \frac{t_2}{2}$ and (b) $t_2^{'} \neq \frac{t_2}{2}$ and the Topological Phase diagram

In Fig. 5, it can be seen IN (a) that in the nontrivial region, when $\mathcal{Z} = 1$, the system hosts the degenerate zero-energy edge states within the bulk states in a wide range of t_1 pointing to a stable topological metal(TM) phase. Since, $\mathcal{Z} = 0$, for the other values of t_1, the system is a trivial insulator. This shows that a phase transition between normal insulator (NI) and TM occurs with a change in t_1. The hidden inversion symmetry is broken in (b), and the degeneracy of edge states is destroyed. The system is either an ordinary insulator or ordinary metal. Also, $\mathcal{Z}$ becomes continuous and is no more a good indicator of any topological features. The topological phase diagram in (c) is shown as functions of t_1 and t_2'. The red areas show the TM phase the grey areas indicate the NI phase.

Local Density of States (LDOS) Fig. 6 provides additional proof of the transition in terms of the variation of the local density of states with energy and unit cell index. In the TM phase in (a), at zero energy, the localised states are positioned at the ends. The edge states coexist with bulk states. A lack of chiral symmetry leads to a difference in the peak intensities. In (b), we witness the NI phase, so the LDOS vanishes at Fermi energy, and the states are extended.

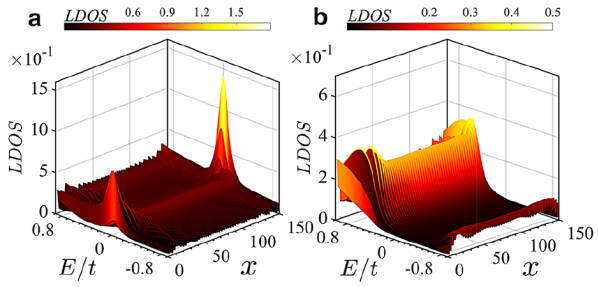

Figure 6: Dependence of local density of states on E and unit cell index x in the (a) TM phase and (b) NI phase

Summary and experimental realisations

The paper satisfactorily discusses a phase transition between a normal insulator and a topological metal in a quasi-1D system. Edge states can be created without chiral or particle-hole symmetry and are protected by the hidden inversion (time-reversal) symmetry.

It is proposed that this theoretical model can be experimentally realised by various systems that display topological features like coupled acoustic resonators, topo-electrical circuits, optical lattices, photonic crystals, and mechanical systems. Quasi-1D chains can also be simulated using cold atoms and spatially resolved density measurements, and spin-resolved time-of-flight imaging for momentum-distribution measurements can be used to reveal topological features. The edge states can also be detected using spatially resolved radio-frequency spectroscopy to probe the LDOS. Furthermore, edge state transport can distinguish between topologically trivial and nontrivial edge states.

The paper is quite detailed in its analysis of the given system but does not provide any applications of this particular model for practical purposes. Its main advantage is the study of the role of hidden symmetries in topological phase transitions. The authors of this paper also published a paper in November 2022 that considers a more general system and concludes that even though chiral, particle-hole or time-reversal symmetry may seem absent from the system, the presence of hidden symmetries in the subspaces of the overall system can also result in topological phases of matter.

2D and 3D topological insulators

The first reported example of 2D topological order was the Quantum Hall effect, where edges are perfect quantum wires wrapped around an insulating droplet. This motivated research in the area of topological materials. Kane and Mele made key theoretical advances in defining topological invariants, which inspired predictions of (Hg, Cd)Te quantum wells being 2D topological insulators by Bernevig, Hughes and Zhang. This was experimentally realised and confirmed by Molenkamp through transport experiments.

The first 3D topological insulator was discovered to be the alloy Bi_xSb_{1-x}. The band structure of Bi_xSb_{1-x} was found to be complicated, and the search began for other topological insulators. A second generation of 3D topological insulator materials was discovered recently in Bi_2Se_3 and Bi_2Te_3. The topological features in 3D materials are determined using angle-resolved photoemission spectroscope (ARPES).

In ARPES experiments, a high-energy photon is used to eject an electron from a crystal. Then the surface or bulk electronic structure is determined from an analysis of the momentum of the emitted electron. It is ideal for probing topological materials because High-resolution ARPES performed with modulated photon energy allows a clear distinction between surface states and the bulk states in the 3D band structure because surface states do not disperse along a direction perpendicular to the surface whereas the bulk states do.

Applications and future scope

- Spin torque device for magnetic memory applications: Heterostructures of topological insulators and ferromagnets can be designed to facilitate switching of ferromagnet by passing current in TI surface
- Magnetoelectric effect and Axion dynamics: Applied electric field generates a magnetic dipole and vice versa in topological materials due to the spin-orbital interaction or axion dynamics. Such materials have the potential advantage over multiferroic materials not in strength but in the increase of speed and reproducibility without fatigue because this effect results purely from the orbital motion of the electrons.
- Emergent particles like Majorana fermions: Topological insulators placed near superconductors can create stable edge states for the emergence of Majorana particles. This presents a possibility for the first direct observation of the particles. Majorana fermions obey special non-abelian quantum statistics and can be used in topological quantum computers well protected from error.